

# Neutrino Tomography of the Earth with Hyper-Kamiokande Detector

S. T. Petcov

INFN/SISSA, Trieste, Italy,  
Kavli IPMU, University of Tokyo, Japan, and  
INRNE, Bulgarian Academy of Sciences, Sofia, Bulgaria

International Workshop “Neutrino Geoscience”  
Kingston, Ontario, Canada  
October 27 - 30, 2025

**Neutrino Tomography of the Earth is one of the most interesting, important and not yet fully explored field of reserach in today's Neutrino Physics.**

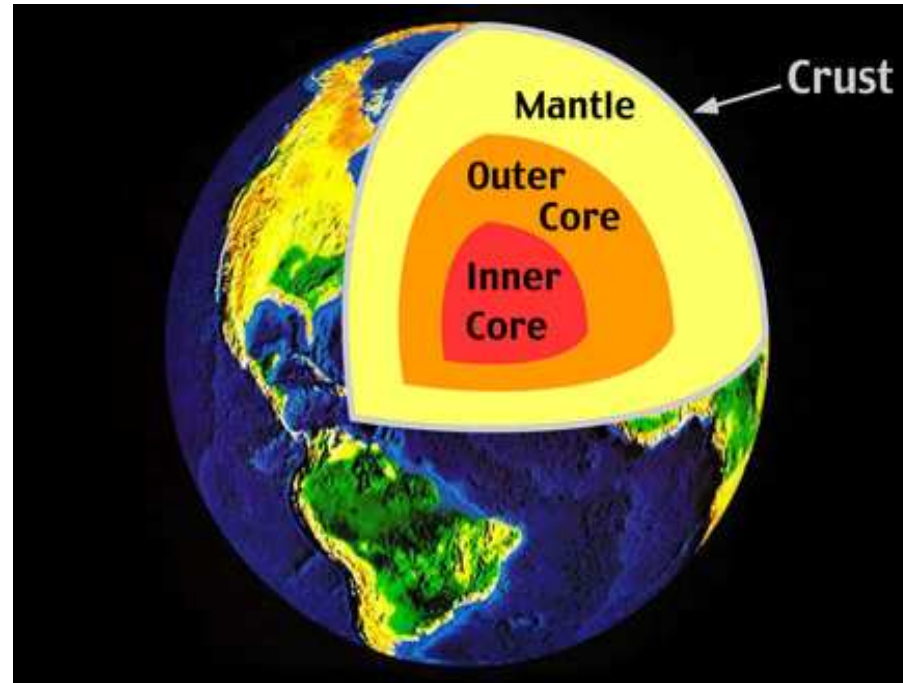
**Two very different methods:  
neutrino absorption tomography and neutrino oscillation tomography.**

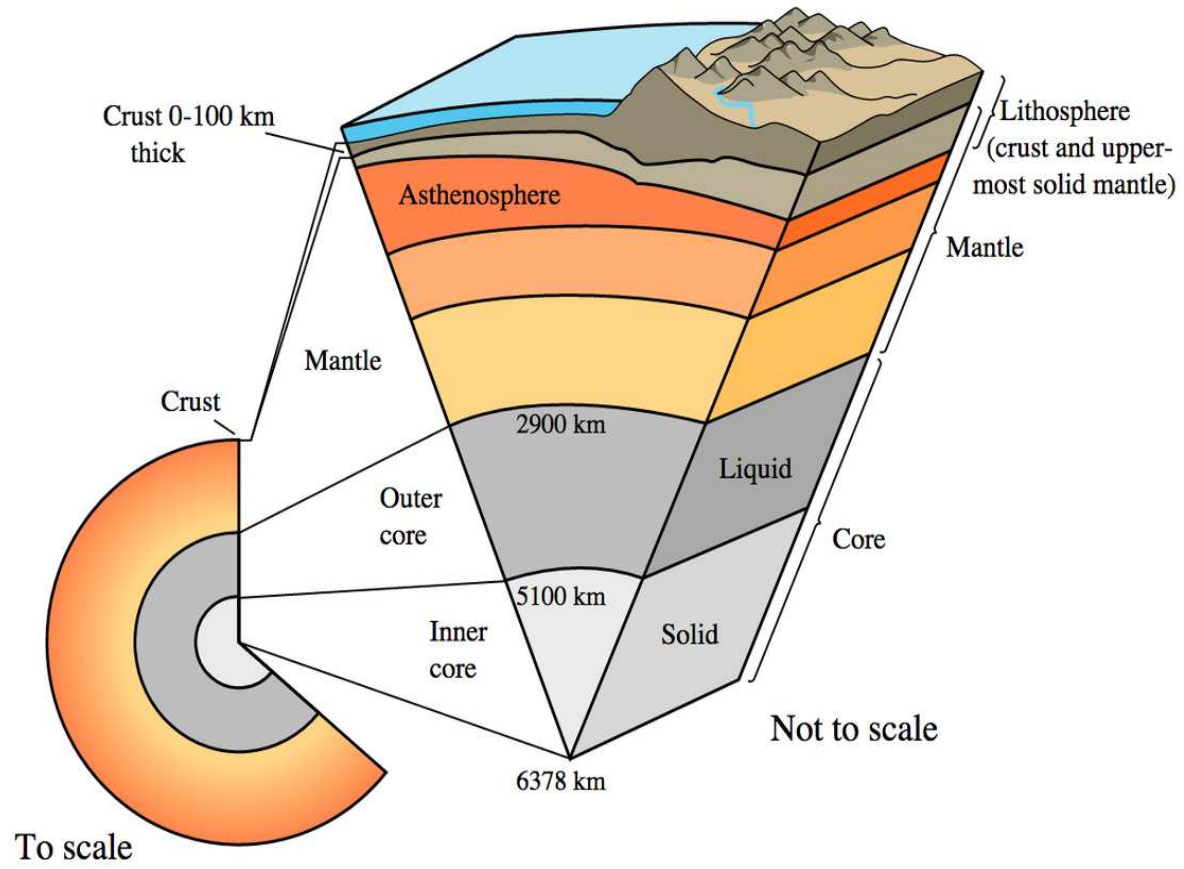
**This talk: Neutrino Oscillation Tomography of the Earth.**

**Can be done with atmospheric, solar and SN neutrinos, in principle.**

**At present, neutrino oscillation tomography of the Earth with atmospheric neutrino seems to be the most feasible in view of the existing and upcoming/planned adequate experiments (KM3NET-ORCA, IceCube-Gen2, JUNO, HK, DUNE, INO).**

# The Earth





At present our knowledge about the interior composition of the Earth and its density structure is based primarily on seismological and geophysical data.

See, e.g., W.F. McDonough, “Treatise on Geochemistry: The Mantle and Core”, vol. 2 (ed. R. W. Carlson, Elsevier-Pergamon, Oxford, 2003), p. 547.  
B.L.N. Kennett, Geophys. J. Int. **132**, 374 (1998);  
G. Masters and D. Gubbins, Phys. Earth Planet. Inter. **140**, 159 (2003).

These data were used to construct the Preliminary Reference Earth Model (PREM) of the density distribution of the Earth: A. M. Dziewonski and D. L. Anderson, “Preliminary reference earth model,” Phys. Earth Planet. Interiors **25** (1981) 297.

In the PREM model,  $\rho_E$  is assumed to be spherically symmetric,  $\rho_E = \rho_E(r)$ ,  $r$  being the distance from the Earth center, and there are three major density structures - the inner core, the outer core and the mantle, and a certain number of substructures (shells or layers). The mantle has five shells in the model. There are three “thin” layers close to the Earth surface: the ocean and the two crust layers (total width  $\sim 100$  km).

The change of  $\rho_E$  ( $N_e$ ) from the mantle to the core and from the outer core to the inner core, according to PREM, can well be approximated by the step function.

# The Earth (PREM)

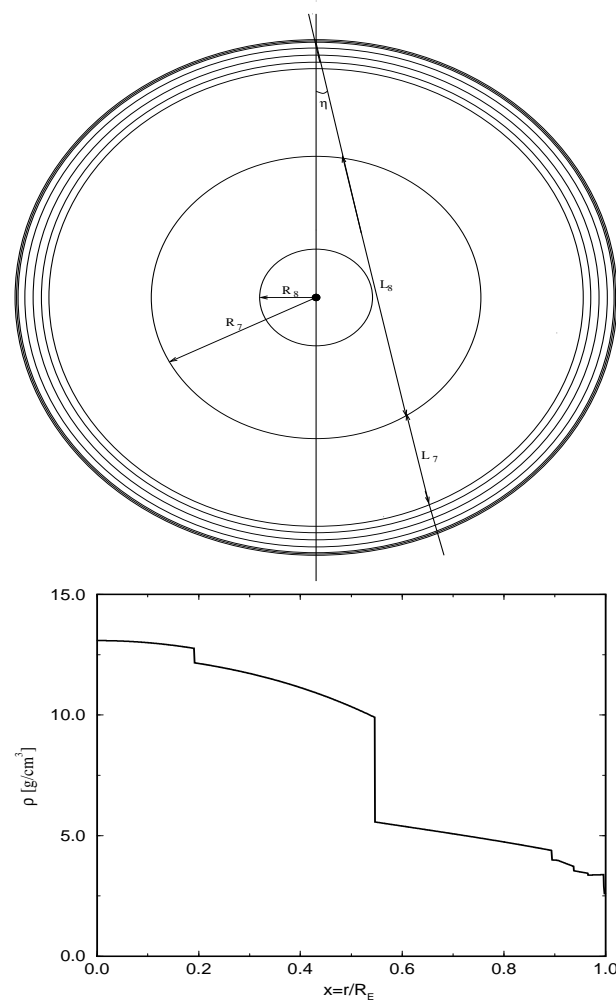
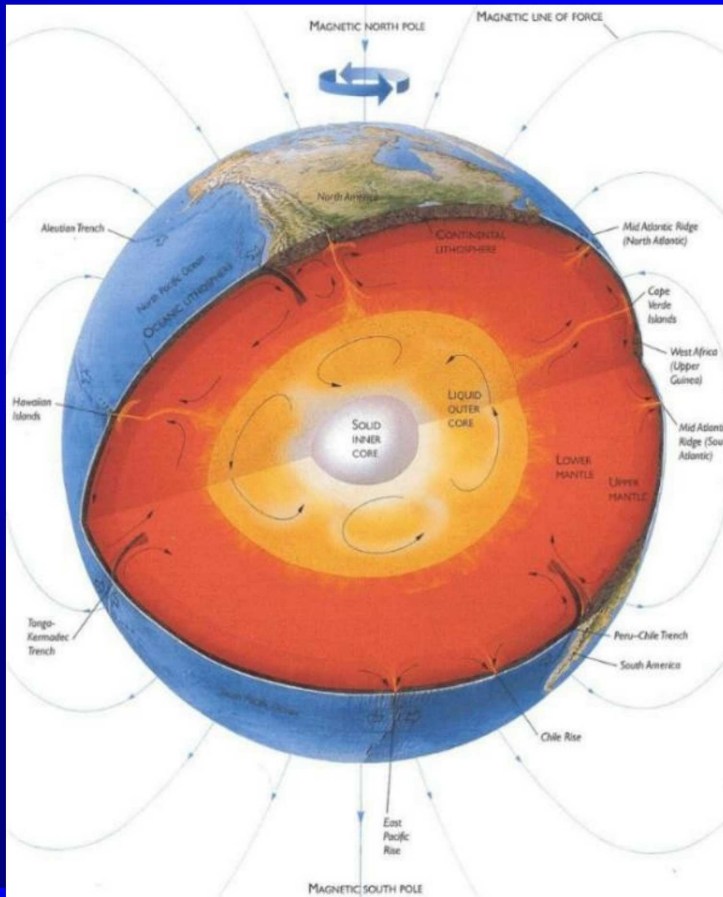


FIG. 1. Density profile of the Earth.

$$R_{\oplus} = 6371 \text{ km}; R_{IC} = 1221.5 \text{ km}; R_C = 3480 \text{ km}; D_{\text{man}} = 2891 \text{ km}; \\ \bar{\rho}_{\text{man}} = 4.45 \text{ g/cm}^3; \bar{\rho}_C = 10.99 \text{ g/cm}^3; \bar{\rho}_{IC}^{16} = 12.89 \text{ g/cm}^3; \bar{\rho}_{OC} = 10.90 \text{ g/cm}^3.$$

# Earth's Core

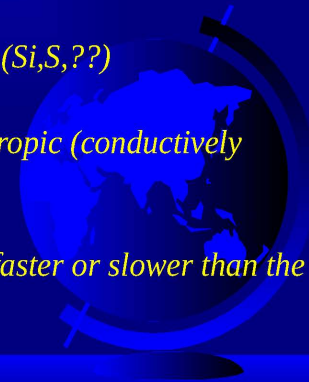


## OUTER CORE

- fluid (viscosity similar to water)
- radius of 3480 km (bigger than Mars)
- ~90% Fe/Ni, 10% (Si, S, ??)

## INNER CORE

- solid-ish (viscosity of  $10^{10-20}$  Pas, Poisson's ratio of 0.42)
- radius of 1221 km (bigger than Pluto)
- ~95% Fe/Ni, 5% (Si, S, ??)
- elastically anisotropic (conductively too ??)
- May be rotating faster or slower than the rest of the Earth



K.D. Koper, talk at the MMTE 2022 workshop (Snowbird, Utah)

Mantle: 44.8% Oxygen, 21.5% Silicon, 22.8% Magnesium + iron, aluminum, calcium, sodium and potassium - all bound together in silicate rocks (in the form of oxides).

**Spherically symmetric  $\rho_E$ : the  $\nu$  trajectory through the Earth is specified by the nadir (zenith) angle  $\theta_n$  (or  $\theta_z$ ).**

**For  $\theta_n \leq 33.17^\circ$ , or path lengths  $L \geq 10660$  km, neutrinos cross the Earth core.**

**The path length for neutrinos which cross only the Earth mantle is given by  $L = 2R_\oplus \cos \theta_n$ ,  $\theta_n$ .**

**If neutrinos cross the Earth core, the lengths of the paths in the mantle,  $2L^{\text{man}}$ , and in the core,  $L^{\text{core}}$ , are determined by:  $L^{\text{man}} = R_\oplus \cos \theta_n - (R_c^2 - R_\oplus^2 \sin^2 \theta_n)^{\frac{1}{2}}$ ,  $L^{\text{core}} = 2(R_c^2 - R_\oplus^2 \sin^2 \theta_n)^{\frac{1}{2}}$ .**

**$\rho_E(r)$  ( $N_e$ ) changes relatively little around the quoted mean values along the trajectories of neutrinos which cross a substantial part of the Earth mantle, or the mantle and the outer core, or the mantle and the outer core and the inner core.**

The determination of the radial density distributions in the mantle and core,  $\rho_{man}(r)$  and  $\rho_c(r)$ , from seismological and geophysical data is not direct and suffers from uncertainties. It is difficult to quantify these uncertainties.

B. A. Bolt, Q. J. R. Astron. Soc. **32**, 367 (1991).

B.L.N. Kennett, Geophys. J. Int. **132**, 374 (1998);

G. Masters and D. Gubbins, Phys. Earth Planet. Inter. **140**, 159 (2003).

It requires the knowledge, in particular, of the seismic wave speed velocity distribution in the interior of the Earth, which depends on the pressure, temperature, composition and elastic properties of the Earth's interior that are not known with a good/high precision.

Often  $\rho_E(r)$  is determined using an empirical relation between the seismic wave velocities and  $\rho_E(r)$  (one example is the Birch law, which may fail at the higher densities of the core) and the so-called “Adams-Williamson equation” (from 1923). E. Williamson and L.H. Adams, J. Wash. Acad. Sci. **13** (1923) 413.

The most precise determination of  $\rho_E(r)$  seems to be achieved by using the data on the low frequency (0.2-10 mHz) normal mode oscillations of the Earth surface following relatively strong earthquakes ( $M_w \sim (8 - 9)$ ).

A. Deuss, talk at MMTE 2023, Paris, France

An approximate and perhaps rather conservative estimate of this uncertainty for  $\rho_{man}(r)$  is  $\sim 5\%$ ; for the core density  $\rho_c(r)$  it is larger and can be significantly larger (Bolt:1991,Kennett:1998,Masters:2003).

**A precise knowledge of  $\rho_E(r)$  and of  $\bar{\rho}_{\text{man}}$ ,  $\bar{\rho}_C$  and  $\bar{\rho}_{\text{IC}}$ , is essential for understanding the physical conditions and fundamental aspects of the structure and properties of the Earth's interior (including the dynamics of mantle and core, the bulk composition of the Earth's three structures, the generation, properties and evolution of the Earth's magnetic field and the gravity field of the Earth) (Bolt:1991, Yoder:1995, McDonough:2003, McDonough:2008zz).**

The thermal evolution of the Earth's core, in particular, depends critically on the density change across the inner core - outer core boundary (see, e.g., Baffet:1991).

**An independent determination of  $\rho_E(r)$  and of  $\bar{\rho}_{\text{man}}$ ,  $\bar{\rho}_C$  and  $\bar{\rho}_{\text{IC}}$ , is highly desirable and would be extremely useful.**

**A unique alternative method of determination of the density profile of the Earth is the neutrino tomography of the Earth.**

The propagation of the active flavour neutrinos and antineutrinos  $\nu_\alpha$  and  $\bar{\nu}_\alpha$ ,  $\alpha = e, \mu, \tau$ , in the Earth is affected by the Earth matter.

The original idea is based on the observation that

**$\sigma(\nu_\alpha(\bar{\nu}_\alpha) + N)$  rises with energy.**

For  $\nu_\alpha, \bar{\nu}_\alpha$  with  $E_\nu \gtrsim$  a few TeV, the inelastic scattering off protons and neutrons leads to absorption of  $\nu$ s and thus to attenuation of the initial  $\nu$  flux.

The magnitude of the attenuation depends on the Earth matter density profile along the neutrino path.

Attenuation data for  $\nu$ s with different path-lengths in the Earth carry information about the matter density distribution in the Earth interior.

The absorption method of Earth tomography **with accelerator neutrino beams, which is difficult (if not impossible) to realise in practice**, was discussed first by Placci and Zavattini in 1973 and Volkova and Zatsepin in 1974, and later in greater detail in Nedyalkov:1981, Nedyalkov:1981yy, Nedyalkov:1982, Nedyalkov:1983, DeRujula:1983ya, Wilson:1983an, Askar:1984, Borisov:1986sm, Borisov:1989kh, Winter:2006vg, Kuo95, Jain:1999kp, Reynoso:2004dt.

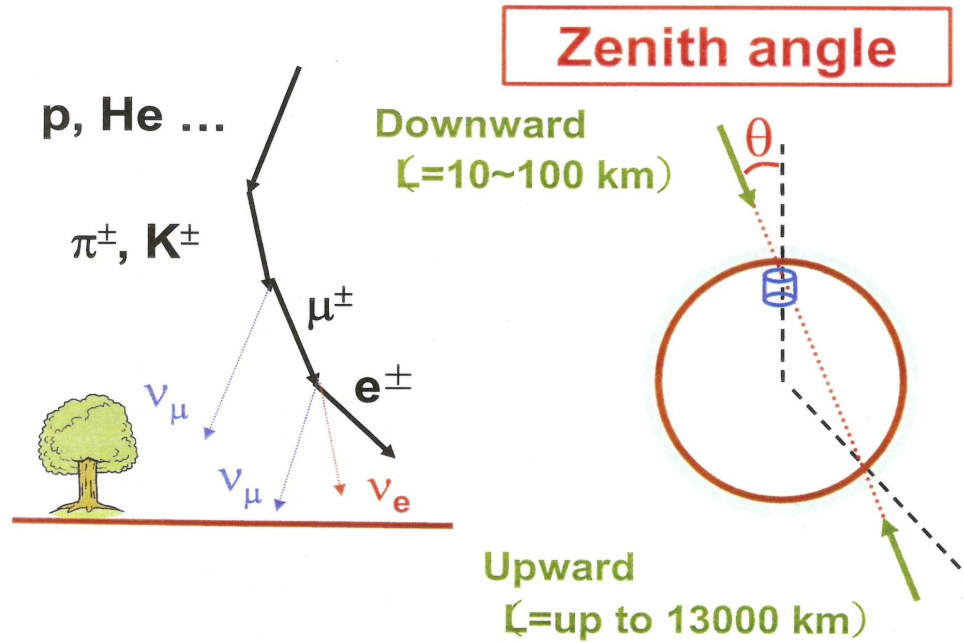
**Atmospheric  $\nu$ s are a perfect tool for performing Earth tomography:**

- i) consist of significant fluxes of  $\nu_\mu$ ,  $\nu_e$ ,  $\bar{\nu}_\mu$  and  $\bar{\nu}_e$ , produced in the interactions of cosmic rays with the Earth atmosphere,
- ii) have a wide range of energies spanning the interval from a few MeV to multi-GeV to multi-TeV,
- iii) being produced isotropically in the upper part of the Earth atmosphere at a height of  $\sim 15$  km, they travel distances from  $\sim 15$  km to 12742 km before reaching detectors located on the Earth surface, crossing the Earth along all possible directions and thus “scanning” the Earth interior.

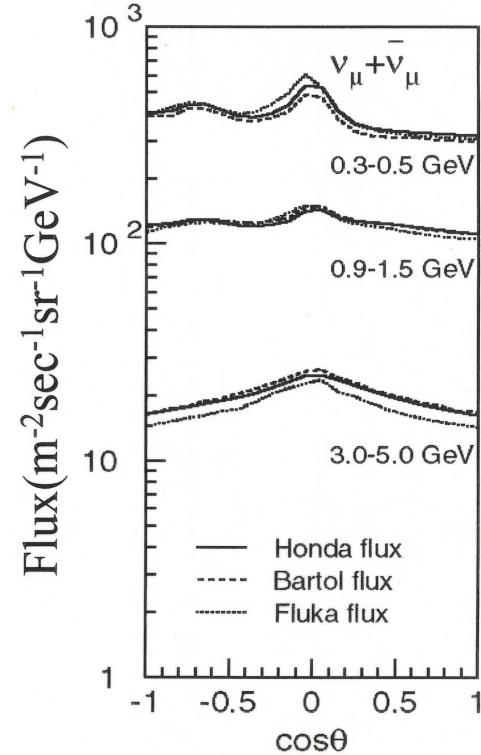
See, e.g., T.K. Gaisser and M. Honda, *Ann. Rev. Nucl. Part. Sci.* **52** (2002) 153  
[arXiv:hep-ph/0203272]

The interaction rates that allow to get information about the Earth density distribution can be obtained in the **currently taking data IceCube experiment and in the experiments ORCA (within the KM3Net project), IceCube-Gen2 and Hyper Kamiokande (HK) and DUNE, which are under construction, in the planned INO experiment and possibly in the JUNO experiment, which started taking data in August, 2025.**

# Atmospheric neutrinos

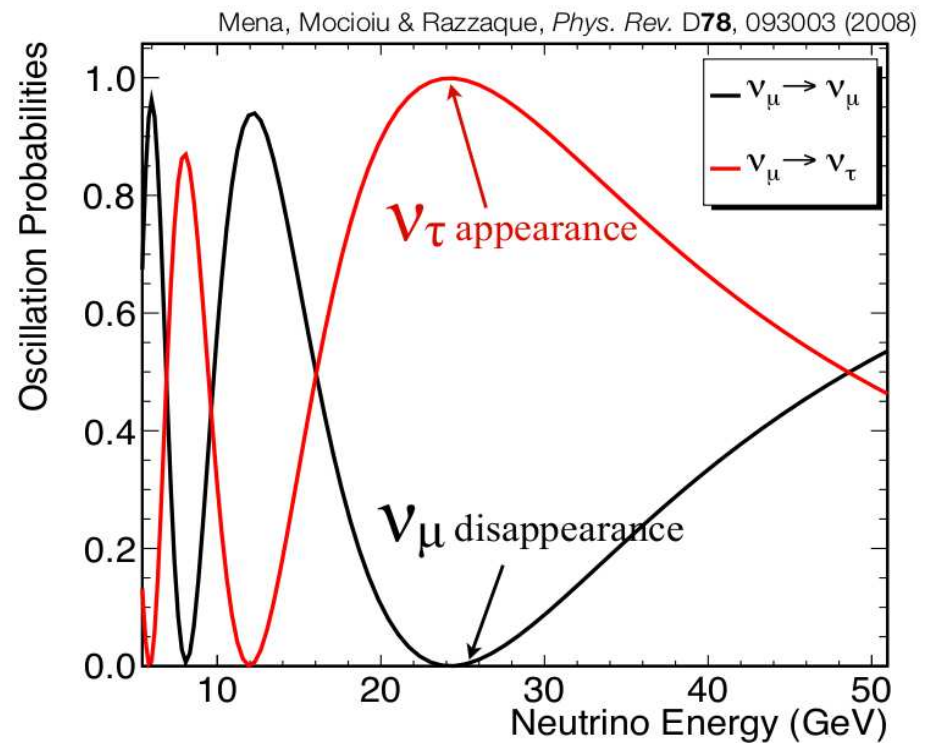
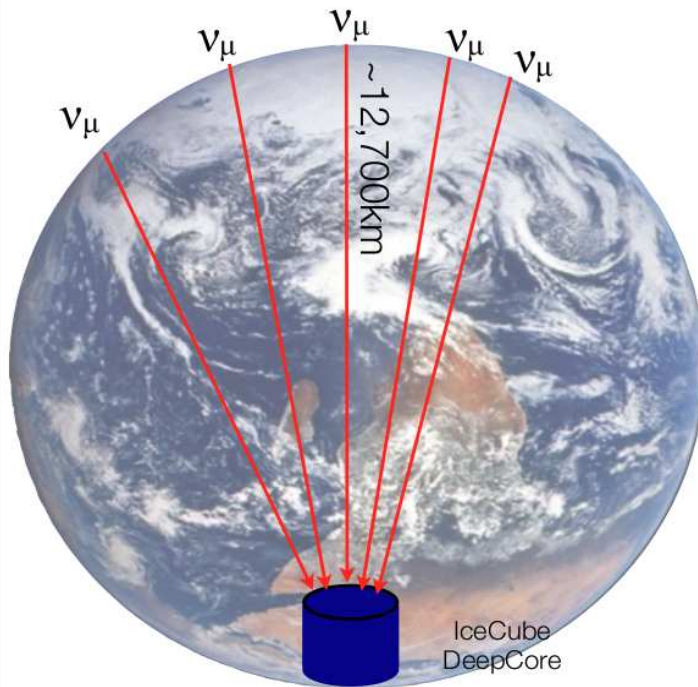


Zenith angle dist. of Atmospheric  $\nu$  flux



$E_\nu > \text{a few GeV}$   
Up/Down Symmetry

- Northern Hemisphere  $\nu_\mu$  oscillating over one earth radii produces  $\nu_\mu$  ( $\nu_\tau$ ) oscillation minimum(maximum) at  $\sim 25$  GeV
  - Covers all possible terrestrial baselines
  - “Beam” is free and never turns off



The idea of using the **absorption method** of Earth tomography with atmospheric neutrinos was discussed first in  
M. C. Gonzalez-Garcia *et al.*, Phys. Rev. Lett. 100 (2008) 061802.

**A. Donini, S. Palomares-Ruiz and J. Salvado, Nature Phys. 15 (2019) 37, using the IceCube zenith angle distribution data on multi-TeV (1.5-20.0 TeV) atmospheric  $\nu_\mu$  and  $\bar{\nu}_\mu$  obtained information about  $\rho_E(r)$ , which, although not very precise, broadly agrees with the PREM model.**

**“Weighted” the Earth with neutrinos:  $M_\oplus^\nu = (6.0_{-1.3}^{+1.6}) \times 10^{24}$  kg,**  
to be compared with the gravitationally determined value:  
 $M_\oplus = (5.9722 \pm 0.0006) \times 10^{24}$  kg.

Marked the beginning of real experimental data driven neutrino tomography of the Earth.

Neutrino oscillation Earth tomography is based on the fact that given the measured  $3 - \nu$  oscillation parameters

$$\Delta m_{21}^2, |\Delta m_{31}^2|, \sin^2 \theta_{12}, \sin^2 \theta_{13}, \sin^2 \theta_{23},$$

for  $E_\nu \sim (2 - 10) \text{ GeV}$  ( $E_\nu \sim 0.2 \text{ GeV}$ , DUNE),

$$P_{3\nu}(\nu_{\mu(e)} \rightarrow \nu_{e(\mu)}) \text{ or } P_{3\nu}(\bar{\nu}_{\mu(e)} \rightarrow \bar{\nu}_{e(\mu)})$$

exhibits a strong dependence on  $\rho_E(r)$  along the  $\nu$  path in the Earth via

$$V_{eff} = \pm \sqrt{2} G_F N_e(r) = \pm \sqrt{2} G_F Y_e \frac{\rho_E(r)}{m_N},$$

$$Y_e = \frac{N_e(r)}{N_p(r) + N_n(r)}$$

**Isotopically symmetric medium:**  $N_e(r) = N_p(r) = N_n(r)$ :  $Y_e = 0.5$ .

$\text{sgn}(\Delta m_{31}^2)$  – not yet determined from data.

$\Delta m_{31}^2 > 0$  (**NO**):  $P_{3\nu}(\nu_{\mu(e)} \rightarrow \nu_{e(\mu)})$  – resonantly enhanced,  $P_{3\nu}(\bar{\nu}_{\mu(e)} \rightarrow \bar{\nu}_{e(\mu)})$  – suppressed.

$\Delta m_{31}^2 < 0$  (**IO**):  $P_{3\nu}(\nu_{\mu(e)} \rightarrow \nu_{e(\mu)})$  – suppressed,  $P_{3\nu}(\bar{\nu}_{\mu(e)} \rightarrow \bar{\nu}_{e(\mu)})$  – resonantly enhanced.

For  $E_\nu \sim (2 - 10)$  **GeV**, effects of  $\Delta m_{21}^2$  and  $\delta_{\text{CP}}$  – subleading.  
( $E_\nu \sim 0.2$  GeV (DUNE),  $\Delta m_{31}^2$  “averaged out” .)

There is a strong dependence of the results on  $\sin^2 \theta_{23}$   
(not precisely measured yet,  $\sin^2 \theta_{23} = (0.42 - 0.58)$  allowed at  $3\sigma$ )  
and on the currently unknown **neutrino mass ordering (NO or IO)**.

$\sin^2 \theta_{23}$ : T2K, NO $\nu$ A, T2HK, DUNE

Neutrino mass ordering (NO or IO): JUNO, ORCA, DUNE, T2HK + HK(atm.  $\nu$  data).

JUNO began physics runs at the end of August, 2025.

HK is under construction and is scheduled to start data-taking in 2028.

DUNE is also under construction.

The neutrino oscillation method is sensitive to changes of  $\rho_E(r)$  over scales  $L \gtrsim L_{\text{osc}}/(2\pi)$ . In the cases of interest  $L_{\text{osc}}/(2\pi) \sim (0.5 - 1.0) \times 10^3$  km.

Thus, very “fine” structures in  $\rho_E(r)$  are difficult (if not impossible) to “resolve.

## Atmospheric $\nu$ experiments (ORCA, IceCube, HK, INO, DUNE)

Of interest:  $\nu_{\mu(e)} \rightarrow \nu_{e(\mu)}$ ,  $\bar{\nu}_{\mu(e)} \rightarrow \bar{\nu}_{e(\mu)}$  oscillations in the Earth ( $E_\nu \gtrsim 2$  GeV).

$$P_{3\nu}(\nu_e \rightarrow \nu_\mu) \cong P_{3\nu}(\nu_\mu \rightarrow \nu_e) \cong s_{23}^2 P_{2\nu}, P_{3\nu}(\nu_e \rightarrow \nu_\tau) \cong c_{23}^2 P_{2\nu},$$
$$P_{3\nu}(\nu_\mu \rightarrow \nu_\mu) \cong 1 - s_{23}^4 P_{2\nu} - 2c_{23}^2 s_{23}^2 [1 - \text{Re}(e^{-i\kappa} A_{2\nu}(\nu_\tau \rightarrow \nu_\tau))],$$

$P_{2\nu} \equiv P_{2\nu}(\Delta m_{31}^2, \theta_{13}; E, \theta_n; N_e)$ : 2- $\nu$   $\nu_e \rightarrow \nu'_\tau$  oscillations in the Earth,  
 $\nu'_\tau = s_{23} \nu_\mu + c_{23} \nu_\tau$ ;  $\Delta m_{21}^2 \ll |\Delta m_{31(32)}^2|$ ,  $E_\nu \gtrsim 2$  GeV;

$\kappa$  and  $A_{2\nu}(\nu_\tau \rightarrow \nu_\tau) \equiv A_{2\nu}$  are known phase and 2- $\nu$  amplitude.

**NO:**  $\nu_{\mu(e)} \rightarrow \nu_{e(\mu)}$  **matter enhanced**,  $\bar{\nu}_{\mu(e)} \rightarrow \bar{\nu}_{e(\mu)}$  - **suppressed**

**IO:**  $\bar{\nu}_{\mu(e)} \rightarrow \bar{\nu}_{e(\mu)}$  **matter enhanced**,  $\nu_{\mu(e)} \rightarrow \nu_{e(\mu)}$  - **suppressed**

**No charge identification (IceCube, KM3NET-ORCA, HK(?)); event rate (DIS regime):**  $[2\sigma(\nu_l + N \rightarrow l^- + X) + \sigma(\bar{\nu}_l + N \rightarrow l^+ + X)]/3$

**Charge identification: INO, DUNE; event rate (DIS regime):**  
 $\sigma(\nu_l + N \rightarrow l^- + X)$ ,  $\sigma(\bar{\nu}_l + N \rightarrow l^+ + X)$

$E_\nu \sim 200$  MeV (**DUNE**):  $P_{3\nu}(\nu_e \rightarrow \nu_\mu) \cong P_{3\nu}(\nu_\mu \rightarrow \nu_e) \cong \cos^2 \theta_{23} \tilde{P}_{2\nu}$ ,  
 $\tilde{P}_{2\nu} \equiv P_{2\nu}(\Delta m_{21}^2, \theta_{12}; E, \theta_n; N_e)$ : 2- $\nu$   $\nu_e \rightarrow \tilde{\nu}'_\tau$  oscillations in the Earth,  
 $\tilde{\nu}'_\tau = c_{23} \nu_\mu - s_{23} \nu_\tau$ .

**All detectors: strong dependence on  $\sin^2 \theta_{23}$  and on neutrino MO.**

**The oscillations  $\nu_\alpha \leftrightarrow \nu_\beta$  and  $\bar{\nu}_\alpha \leftrightarrow \bar{\nu}_\beta$ ,  $\alpha, \beta = e, \mu$ , having  $E \sim (0.1 - 15.0)$  GeV and traversing the Earth can be strongly modified by the Earth matter effects.** These modifications depend on the Earth matter density (more precisely, the electron number density  $N_e(r)$ , see further) along the path of the  $\nu$ s. Thus, by studying the effects of Earth matter on the oscillations of, e.g.,  $\nu_\mu$  and  $\nu_e$  ( $\bar{\nu}_\mu$  and  $\bar{\nu}_e$ ) neutrinos traversing the Earth along different trajectories it is possible to obtain information about the Earth (electron number) density distribution.

The Earth tomography based on the study of the effects of Earth matter on the oscillations of atmospheric neutrinos with different path-lengths in the Earth is discussed in:

S. K. Agarwalla *et al.*, arXiv:1212.2238 (IceCube/DeepCore, PINGU;  $M_{\oplus}$  and EHSE constraints not accounted for).

W. Winter, Nucl. Phys. B 908 (2016) 250 (PINGU, ORCA; 7 layers, densities in these layers varied independently;  $M_{\oplus}$  and EHSE constraints not taken into account; systematic errors “optimistic” (ORCA)).

S. Bouret *et al.* [KM3NeT], J. Phys. Conf. Ser. 888 (2017) 012114 (ORCA; systematic errors not accounted for).

A. Kumar and S. Kumar Agarwalla, JHEP 08 (2021) 139 (INO).

K. J. Kelly, P. A. N. Machado, I. Martinez-Soler and Y. F. Perez-Gonzalez, JHEP 05 (2022) 187 (DUNE).

D. Raikwal and S. Choubey, arXiv:2309.12573 (INO).

#### Early studies:

S. Choubey, P. Ghoshal and S.T.P., studies performed in the period 2008 - 2011 (HK, LAr), unpublished.

S. Choubey and S.T.P., studies performed in 2014 (PINGU), unpublished.

#### Composition of the Earth core ( $N_e$ ):

C. Rott, A. Taketa and D. Bose, Sci. Rep. 5 (2015) 15225 (generic detector).

S. Bouret *et al.*, PoS ICRC2019 (2020) 1024 (ORCA).

## Neutrino Oscillations in Matter (Earth mantle)

When neutrinos propagate in matter, they interact with the background of electrons, protons and neutrons, which generates an effective potential in the neutrino Hamiltonian:  $H = H_{vac} + V_{eff}$ .

This modifies the neutrino mixing since the eigenstates and the eigenvalues of  $H_{vac}$  and of  $H = H_{vac} + V_{eff}$  are different, leading to a different oscillation probability w.r.t to that in vacuum.

Typically the matter background is not CP and CPT symmetric, e.g., the Earth and the Sun contain only electrons, protons and neutrons, and **the resulting oscillations violate CP and CPT symmetries.**

$E_\nu \gtrsim 2 \text{ GeV}$ ,  $\theta_n > 33.17^\circ$  (mantle crossing)

$$P_{3\nu}(\nu_\mu \rightarrow \nu_e) \cong \sin^2 \theta_{23} \sin^2 2\theta_{13}^m \sin^2 \frac{\Delta M_{31}^2 L}{4E}$$

$\sin^2 2\theta_{13}^m$ ,  $\Delta M_{31}^2$  depend on the matter potential  
 $V_{eff} = \sqrt{2} G_F N_e$ ,

For antineutrinos  $V_{eff}$  has the opposite sign:

$$V_{eff} = -\sqrt{2} G_F N_e.$$

$\Delta m_{31}^2 > 0$  (NO):  $\nu_{\mu(e)} \rightarrow \nu_{e(\mu)}$  matter enhanced,  
 $\bar{\nu}_{\mu(e)} \rightarrow \bar{\nu}_{e(\mu)}$  - suppressed

$\Delta m_{31}^2 < 0$  (IO):  $\bar{\nu}_{\mu(e)} \rightarrow \bar{\nu}_{e(\mu)}$  matter enhanced,  
 $\nu_{\mu(e)} \rightarrow \nu_{e(\mu)}$  - suppressed

$$\sin^2 2\theta_{13}^m = \frac{\tan^2 2\theta_{13}}{\left(1 - \frac{N_e}{N_e^{res}}\right)^2 + \tan^2 2\theta_{13}},$$

$$\cos 2\theta_{13}^m = \frac{1 - N_e/N_e^{res}}{\sqrt{\left(1 - \frac{N_e}{N_e^{res}}\right)^2 + \tan^2 2\theta_{13}}},$$

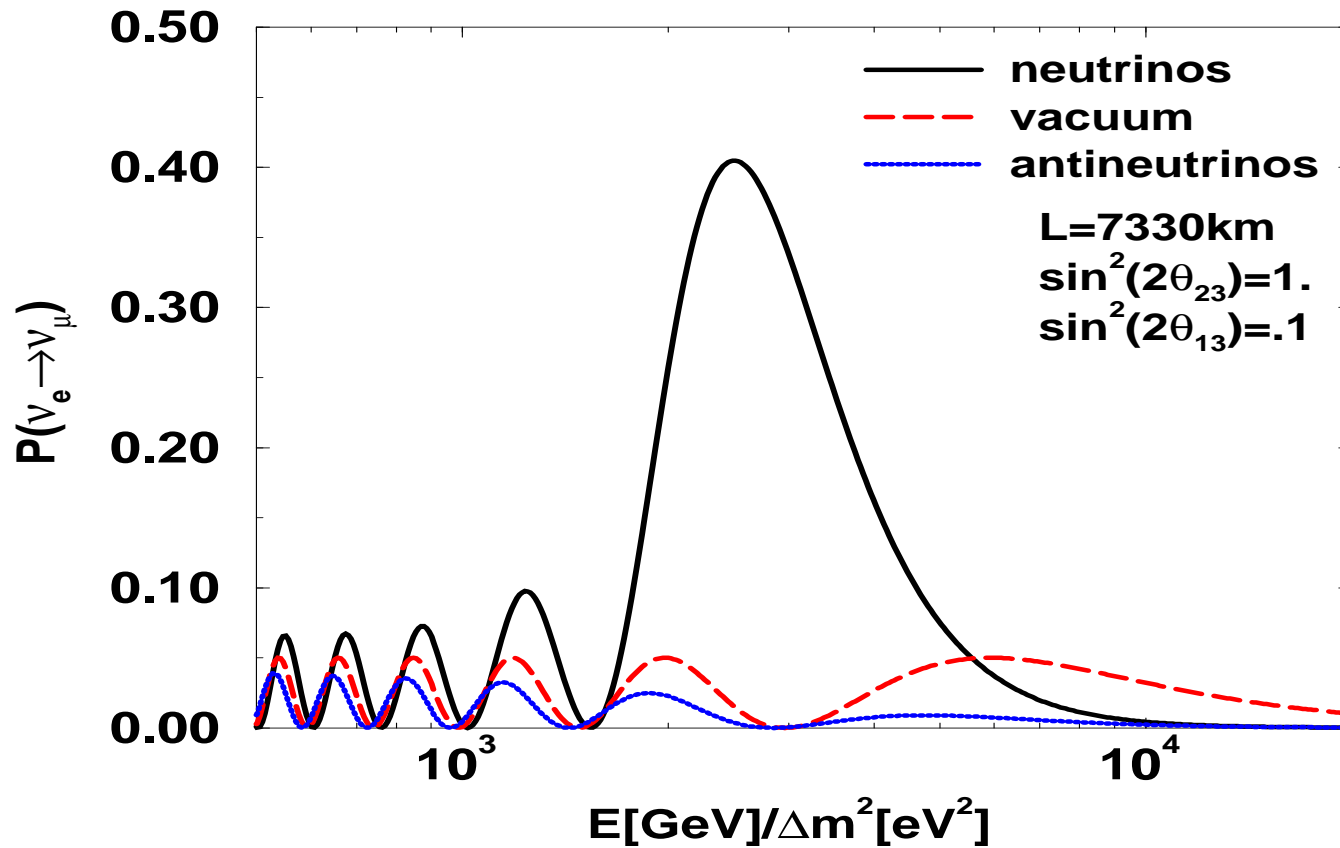
$$N_e^{res} = \frac{\Delta m_{31}^2 \cos 2\theta_{13}}{2E\sqrt{2}G_F},$$

$$N_e^{res} \cong 6.56 \times 10^6 \frac{\Delta m^2 [\text{eV}^2]}{E [\text{MeV}]} \cos 2\theta_{13} \text{ cm}^{-3} N_A,$$

$$\frac{\Delta M_{31}^2}{2E} \equiv \frac{\Delta m_{31}^2}{2E} \left( \left(1 - \frac{N_e}{N_e^{res}}\right)^2 \cos^2 2\theta_{13} + \sin^2 2\theta_{13} \right)^{\frac{1}{2}}$$

For  $\bar{\nu}_\mu \rightarrow \bar{\nu}_e$ :  $N_e \rightarrow (-N_e)$ .

# Earth matter effect in $\nu_\mu \rightarrow \nu_e, \bar{\nu}_\mu \rightarrow \bar{\nu}_e$ in the mantle (MSW)



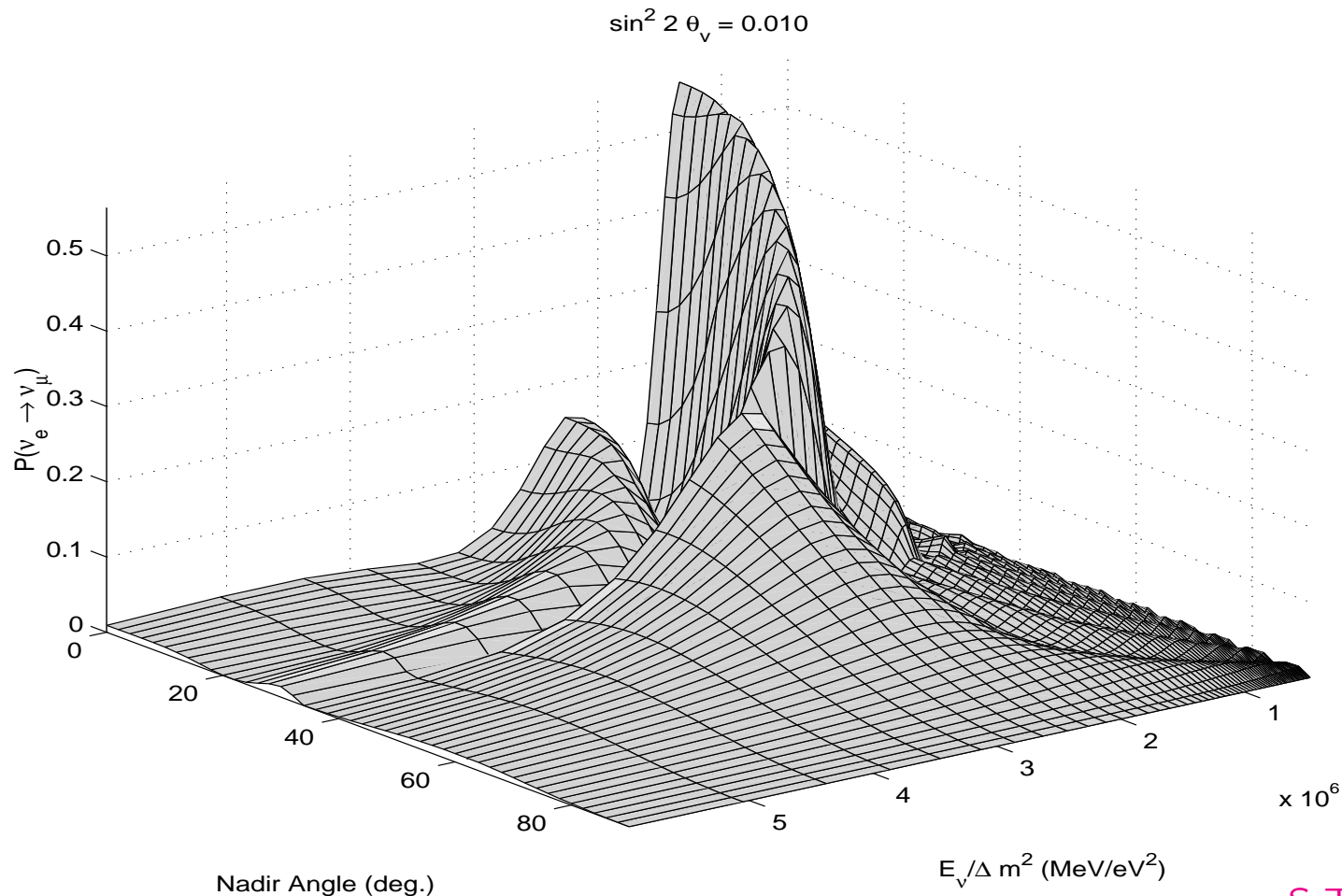
I. Mocioiu, R. Shrock, 2000

$\Delta m_{31}^2 = 2.5 \times 10^{-3} \text{ eV}^2$ ,  $E^{res} = 6.25 \text{ GeV}$ ;  $P^{3\nu} = \sin^2 \theta_{23} P_m^{2\nu} = 0.5 P_m^{2\nu}$ ;  
 Maximum at  $\rho^{res} = ((\Delta m_{31}^2 \cos 2\theta_{13}) / (2E\sqrt{2}G_F))(m_N/Y_e) = \bar{\rho}_{man} \cong 4.6 \text{ g/cm}^{-3}$ ,  
 $L_m^{res} = L^v / \sin 2\theta_{13} \cong 6250 / 0.32 \text{ km}$ ;  $2\pi L / L_m \cong 0.75\pi (\neq \pi)$ ..

**Sensitivity to  $\bar{\rho}_{man}$  along the  $\nu$  path in the mantle.**

# Resonance-like Amplification of Oscillations of Neutrinos Crossing the Earth Core

# Earth matter effects in $\nu_\mu \rightarrow \nu_e, \bar{\nu}_\mu \rightarrow \bar{\nu}_e$ (NOLR)



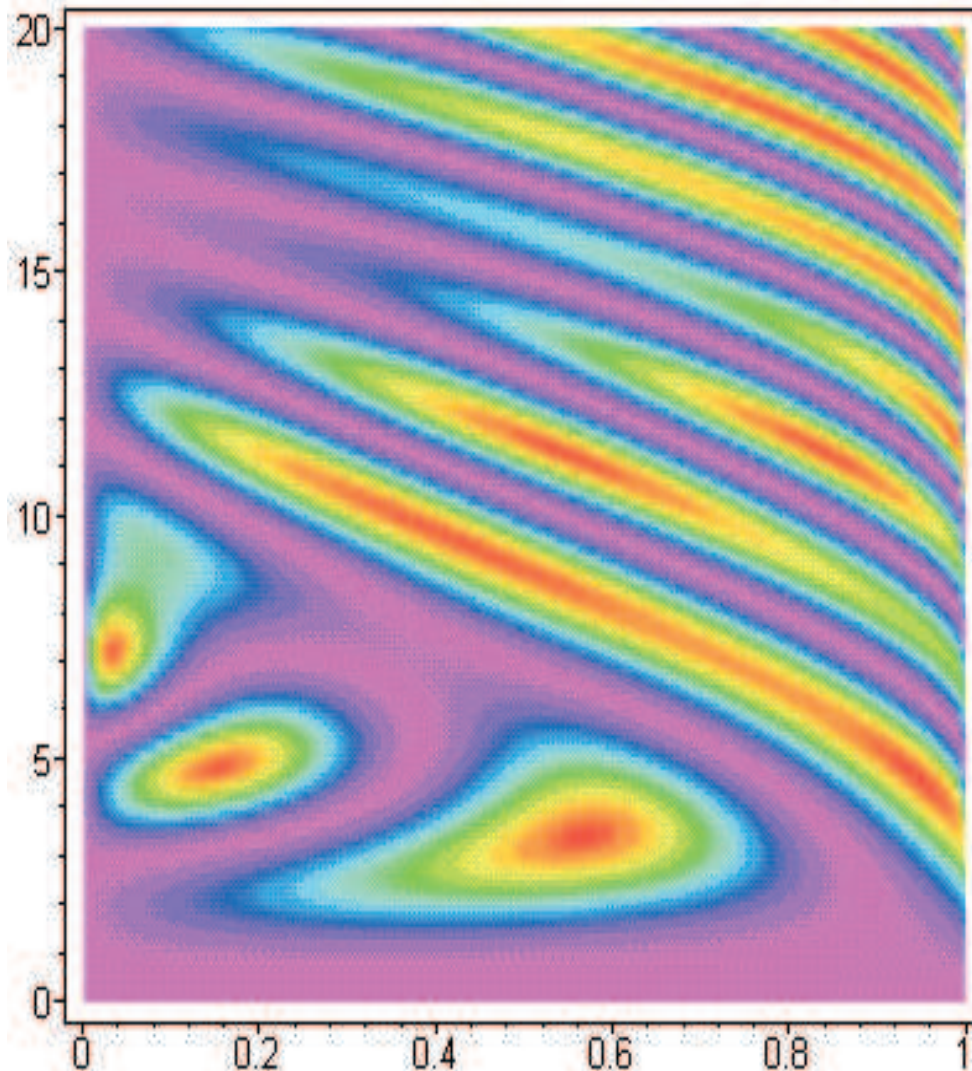
S.T.P., 1998;  
M. Chizhov, M. Maris, S.T.P., 1998; M. Chizhov, S.T.P., 1999

$P(\nu_e \rightarrow \nu_\mu) \equiv P_{2\nu} \equiv (s_{23})^{-2} P_{3\nu}(\nu_{e(\mu)} \rightarrow \nu_{\mu(e)})$ ,  $\theta_\nu \equiv \theta_{13}$ ,  $\Delta m^2 \equiv \Delta m_{31}^2 > 0$ ;

**Absolute maximum: Neutrino Oscillation Length Resonance (NOLR) :**

$\rho_{man} < \rho^{res} < \rho_{core}$  (NOLR  $\neq$  MSW), sensitivity to  $\bar{\rho}_{man}$ ,  $\bar{\rho}_{core}$ .

**Local maxima: MSW effect in the Earth mantle or core.**



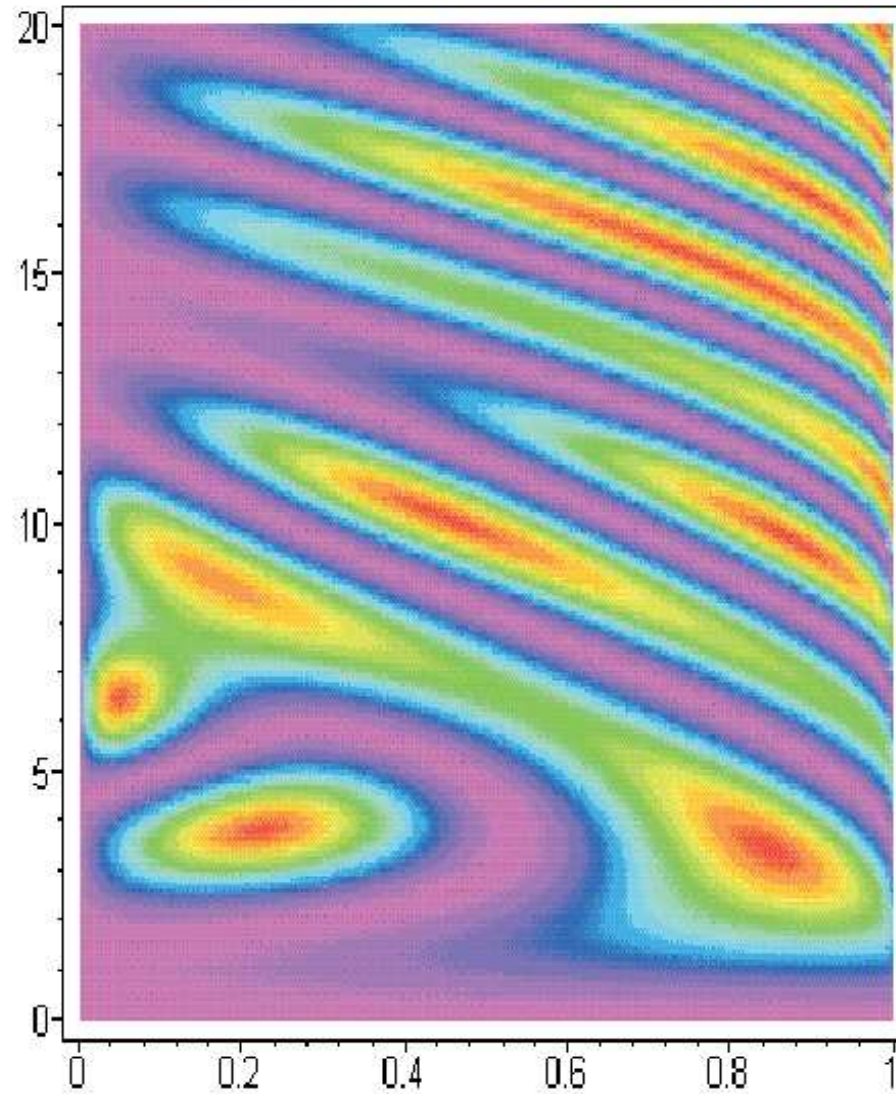
$(s_{23})^{-2} P_{3\nu}(\nu_{e(\mu)} \rightarrow \nu_{\mu(e)}) \equiv P_{2\nu}$ ; **“Dark Red Spots”**,  $P_{2\nu} = 0.9 - 1.0$ ;

**NOLR:**  $P_{2\nu} = 1$  at  $\sin^2 2\theta_{13} = 0.034$ ;  $0.154$ ,  $E \cong 3.5$ ;  $5.2$  **GeV**.

**Vertical axis:**  $\Delta m^2/E$  [ $10^{-7} \text{eV}^2/\text{MeV}$ ]; **horizontal axis:**  $\sin^2 2\theta_{13}$ ;  $\theta_n = 0$

M. Chizhov, S.T.P., 1999 (hep-ph/9903399,9903424)

**Sensitivity to  $\bar{\rho}_{\text{man}}$ ,  $\bar{\rho}_{\text{Core}}$ , and to  $(\bar{\rho}_{\text{Core}}/\bar{\rho}_{\text{man}})_{mcb}$  at mantle-core boundary.**



The same for  $\theta_n = 23^\circ$ .

**Vertical axis:**  $\Delta m^2/E$  [ $10^{-7} eV^2/MeV$ ]; **horizontal axis:**  $\sin^2 2\theta_{13}$ .

M. Chizhov, S.T.P., 1999 (hep-ph/9903399,9903424)

- For Earth center crossing  $\nu$ 's ( $\theta_n = 0$ ) and, e.g.  $\sin^2 2\theta_{13} = 0.01$ , **NOLR** occurs at  $E \cong 4$  **GeV** ( $\Delta m^2(atm) = 2.5 \times 10^{-3} \text{ eV}^2$ ).

S.T.P., hep-ph/9805262

- For the Earth core crossing  $\nu$ 's:  $P_{2\nu} = 1$  **due to NOLR** when

$$\tan \Phi^{\text{man}}/2 \equiv \tan \phi' = \pm \sqrt{\frac{-\cos 2\theta''_m}{\cos(2\theta''_m - 4\theta'_m)}},$$

$$\tan \Phi^{\text{core}}/2 \equiv \tan \phi'' = \pm \frac{\cos 2\theta'_m}{\sqrt{-\cos(2\theta''_m) \cos(2\theta''_m - 4\theta'_m)}}$$

$\Phi^{\text{man}}$  ( $\Phi^{\text{core}}$ ) - phase accumulated in the Earth mantle (core),  
 $\theta'_m$  ( $\theta''_m$ ) - the mixing angle ( $\theta_{13}$ ) in the Earth mantle (core).

$P_{2\nu} = 1$  **due to NOLR** for  $\theta_n = 0$  (Earth center crossing  $\nu$ 's) at, e.g.  $\sin^2 2\theta_{13} = 0.034; 0.154$ ,  $E \cong 3.5; 5.2$  **GeV** ( $\Delta m^2(atm) = 2.5 \times 10^{-3} \text{ eV}^2$ ).

For  $E = 3.5$  **GeV**, the probability  $P_{2\nu} \gtrsim 0.5$  for the values of  $\sin^2 2\theta_{13}$  from the interval  $0.02 \lesssim \sin^2 2\theta_{13} \lesssim 0.10$ .

The current b.f.v. of  $\sin^2 2\theta_{13} = 0.084$ .

M. Chizhov, S.T.P., Phys. Rev. Lett. 83 (1999) 1096 (hep-ph/9903399); Phys. Rev. Lett. 85 (2000) 3979 (hep-ph/0504247); Phys. Rev. D63 (2001) 073003 (hep-ph/9903424).

- The first “oscillogram of the Earth” type figures appeared in M. Chizhov, M. Maris, S.T.P., hep-ph/9810501.

The Earth matter effects in  $\nu_{e(\mu)} \rightarrow \nu_{\mu(e)}$ ,  $\bar{\nu}_{e(\mu)} \rightarrow \bar{\nu}_{\mu(e)}$ ,  $\nu_e \rightarrow \nu_\tau$  and  $\bar{\nu}_e \rightarrow \bar{\nu}_\tau$  oscillations are significant for  $E_\nu \sim (2 - 10)$  **GeV**.

**MSW in the Mantle:**  $E_\nu \sim (6 - 7)$  **GeV** ( $|\Delta m_{31}^2| \equiv \Delta m^2(atm) = 2.5 \times 10^{-3}$  eV<sup>2</sup>).

The mantle-core (NOLR) enhancement of  $P_m^{2\nu}$  (or  $\bar{P}_m^{2\nu}$ ):

$P_{2\nu} = 1$  **due to NOLR** for  $\theta_n = 0$  (Earth center crossing  $\nu$ 's) at,  
e.g.  $\sin^2 2\theta_{13} = 0.034; 0.154$ ,  $E \cong 3.5; 5.2$  **GeV** ( $|\Delta m_{31}^2| = 2.5 \times 10^{-3}$  eV<sup>2</sup>).

For  $E = 3.5$  **GeV**, the probability  $P_{2\nu} \gtrsim 0.5$  for the values of  $\sin^2 2\theta_{13}$  from the interval  $0.02 \lesssim \sin^2 2\theta_{13} \lesssim 0.10$ .

The current b.f.v. of  $\sin^2 2\theta_{13} = 0.084$ .

The effects of Earth matter on the oscillations of atmospheric (and accelerator) neutrinos have not been observed so far; **can be used for performing tomography of the Earth with neutrinos having  $E_\nu \sim (2 - 10)$  GeV (DUNE:  $E_\nu \sim 0.2$  GeV, K.J. Kelly et al., arXiv:2110.00003, requires detection of protons in  $\nu_{\mu(e)} + n \rightarrow \mu^-(e^-) + p$ ).**

The fluxes of atmospheric  $\nu_{e,\mu}$  of energy  $E$ , which reach the detector after crossing the Earth along a given trajectory specified by the value of  $\theta_n$ ,  $\Phi_{\nu_{e,\mu}}(E, \theta_n)$ , are given by the following expressions in the case of the 3-neutrino oscillations under discussion and  $E_\nu \gtrsim 2$  GeV:

$$\Phi_{\nu_e}(E, \theta_n) \cong \Phi_{\nu_e}^0 (1 + [s_{23}^2 r - 1] P_m^{2\nu}),$$

$$\Phi_{\nu_\mu}(E, \theta_n) \cong \Phi_{\nu_\mu}^0 (1 + s_{23}^4 [(s_{23}^2 r)^{-1} - 1] P_m^{2\nu} - 2c_{23}^2 s_{23}^2 [1 - \text{Re} (e^{-i\kappa} A_m^{2\nu}(\nu_\tau \rightarrow \nu_\tau))]) ,$$

where  $\Phi_{\nu_{e(\mu)}}^0 = \Phi_{\nu_{e(\mu)}}^0(E, \theta_n)$  is the  $\nu_{e(\mu)}$  flux in the absence of neutrino oscillations and

$$r \equiv r(E, \theta_n) \equiv \frac{\Phi_{\nu_\mu}^0(E, \theta_n)}{\Phi_{\nu_e}^0(E, \theta_n)} .$$

$$r = 2, s_{23}^2 = 0.5: [s_{23}^2 r - 1] = 0$$

$s_{23}^2$ : **b.f.v. 0.455 (0.569) NO (IO);  $3\sigma$  CL: (0.416 (0.417)-0.599 (0.606) .**

F. Capozzi et al., 2107.00532; M.C. Gonzalez-Garcia et al., 2111.03086

$r(E, \theta_n) \cong (2.6 \div 4.5)$  for neutrinos giving the main contribution to the multi-GeV samples,  $E \cong (2 \div 10)$  GeV.

M. Honda, 1995.

**$E_\nu \sim 0.2$  GeV,  $r = 2$ :**

$$\Phi_{\nu_e}(E, \theta_n) \cong \Phi_{\nu_e}^0 (1 + [c_{23}^2 r - 1] P_m^{2\nu}) \cong \Phi_{\nu_e}^0, \text{ if } c_{23}^2 = 0.5 .$$

The Earth matter effects in the  $\nu_{\mu(e)} \rightarrow \nu_{e(\mu)}$  ( $\bar{\nu}_{\mu(e)} \rightarrow \bar{\nu}_{e(\mu)}$ ) oscillations depend on

$$V = \begin{pmatrix} + \\ - \end{pmatrix} \sqrt{2} G_F N_e^{(E)}(r)$$

$$N_e^{(E)}(r) = \rho_E(r) Y_e / m_N,$$

$Y_e$  - electron fraction number (or  $Z/A$  factor).

For isotopically symmetric matter  $Y_e = 0.5$ .

Earth core composition models:  $Y_e^c = 0.466 - 0.471$ .

Earth mantle composition models:  $Y_e^{man} = 0.490 - 0.496$ .

Varying  $Y_e^c$  and  $Y_e^{man}$  in the indicated respective intervals has no effect on the results on the  $\bar{\rho}_{man}$ ,  $\bar{\rho}_C$ ,  $\bar{\rho}_{OC}$ ,  $\bar{\rho}_{IC}$  determination using the neutrino oscillation tomography method.

Determining the composition of, e.g., the OC or IC is technically a very different problem with respect to determining  $\bar{\rho}_{man}$ ,  $\bar{\rho}_C$ ,  $\bar{\rho}_{OC}$ ,  $\bar{\rho}_{IC}$ : **does not require varying  $\bar{\rho}_i$  in the study.**

# Important Constraints

The total Earth mass constraint:

$$M_{\oplus} = (5.9722 \pm 0.0006) \times 10^{24} \text{ kg}$$

Earth momentum of inertia constraint:

$$I_{\oplus} = (8.01736 \pm 0.00097) \times 10^{37} \text{ kg m}^2.$$

$$I_{\oplus} = 0.330745 M_{\oplus} R_{\oplus}^2.$$

Earth hydrostatic equilibrium (EHSE) constraint:

$$\rho_{man} < \rho_{OC} < \rho_{IC}, \text{ or, for example,}$$

$$\rho_{uman} < \rho_{lman} < \rho_{OC} < \rho_{IC}$$

# Neutrino Oscillation Tomography of the Earth with the Hyper-Kaiokande Detector

C. Jesús-Valls, S.T.P., J. Xia, EPJ C85 (2025) 703 [arXiv:2411.12344]

Disclaimer: this study is not a study by the Hyper-Kamiokande collaboration.

## Aspects of the Analysis

We change the **PREM** density in a given layer  $\rho_i(r)$ ,  $i = \text{IC, OC, man}$ , by a factor  $(1 + \kappa_i)$ ,  $\kappa_i$  is  $r$ -independent real constant:

$$\rho_i(r) \rightarrow \rho'_i(r) = (1 + \kappa_i)\rho_i(r).$$

We will present results on sensitivity of HK to

$$\Delta\rho_i = 100\% ((1 + \kappa_i)\rho_i(r) - \rho_i(r))/\rho_i(r) = 100\% \kappa_i.$$

When we increase (decrease) the density in one layer, **in order to keep  $M_\oplus$  and  $I_\oplus$  unchanged**, we have to decrease (increase) the density in at least two other layers. The factor by which that has to be done depends on the relative volumes and densities of the layers. In our study we have accounted for both the  $M_\oplus$  and  $I_\oplus$  constraints when varying  $\rho_i(r)$ .

To be more specific, in the standard 3-layer model of the Earth, consisting of mantle, outer core and inner core, when we consider, e.g., variation of  $\bar{\rho}_{OC}$ , we compensate it by the corresponding change of density of the inner core  $\bar{\rho}_{IC}$  and of the mantle  $\bar{\rho}_{man}$ .

Using the PREM average densities we have:

$$M_{\oplus} = M_{\oplus}(\bar{\rho}'_{IC}, \bar{\rho}'_{OC}, \bar{\rho}'_{man}) = M_{\oplus}(\kappa_{IC}, \kappa_{OC}, \kappa_{man}),$$
$$I_{\oplus} = I_{\oplus}(\bar{\rho}'_{IC}, \bar{\rho}'_{OC}, \bar{\rho}'_{man}) = I_{\oplus}(\kappa_{IC}, \kappa_{OC}, \kappa_{man}) ,$$

i.e., two equations for three unknowns. We can express, e.g.,  $\kappa_{IC}$  and  $\kappa_{man}$  in terms of  $\kappa_{OC}$ .

By using the EHE constraint  $\bar{\rho}'_{man} < \bar{\rho}'_{OC} < \bar{\rho}'_{IC}$  we can obtain the ranges of variation of  $\kappa_{OC}$ , and consequently of  $\kappa_{IC}$  and  $\kappa_{man}$  that are allowed by the  $M_{\oplus}$ ,  $I_{\oplus}$  and EHE constraints.

Numerically we find:

$$-0.018 \text{ (0.036)} \lesssim \kappa_{OC} < 0.010 .$$

S.T.P., 2406.13727

These very restrictive constraints can be traced to the relatively small contributions of the inner core to  $M_{\oplus}$  and especially to  $I_{\oplus}$ . **The observation of such small variations of  $\kappa_{OC}$  is beyond the reach of all currently running, under construction and planned experiments.**

Therefore we have considered the case of two different mantle layers and the core layer. The mantle is divided into

i) **lower mantle**, extending from  $R_c = 3480$  km to  $R_{\text{lman}} = 5701$  km, with PREM density  $\bar{\rho}_{\text{lman}} = 4.9035$  g/cm<sup>3</sup>, and

ii) **upper mantle**, extending from  $R_{\text{lman}} = 5701$  km to  $R_{\text{man}} = 6346.6$  km, with PREM density  $\bar{\rho}_{\text{uman}} = 3.6046$  g/cm<sup>3</sup>.

One finds that in this case the  $M_{\oplus}$ ,  $I_{\oplus}$  and the EHE constraint in the form  $\bar{\rho}'_{\text{uman}} < \bar{\rho}'_{\text{lman}} < \bar{\rho}'_c$  lead to:

- $0.33 < \kappa_c < 0.09$ ,  $7.36 < \bar{\rho}'_c < 11.98$  g/cm<sup>3</sup>,
- $0.13 < \kappa_{\text{lman}} < 0.48$ ,  $4.26 < \bar{\rho}'_{\text{lman}} < 7.25$  g/cm<sup>3</sup>,
- $0.69 < \kappa_{\text{uman}} < 0.18$ ,  $1.12 < \bar{\rho}'_{\text{uman}} < 4.23$  g/cm<sup>3</sup>.

S.T.P., 2406.13727; C. Jesus-Valls, S.T.P., J.Xia, 2411.12344

**We have implemented these constraints in our analysis.**

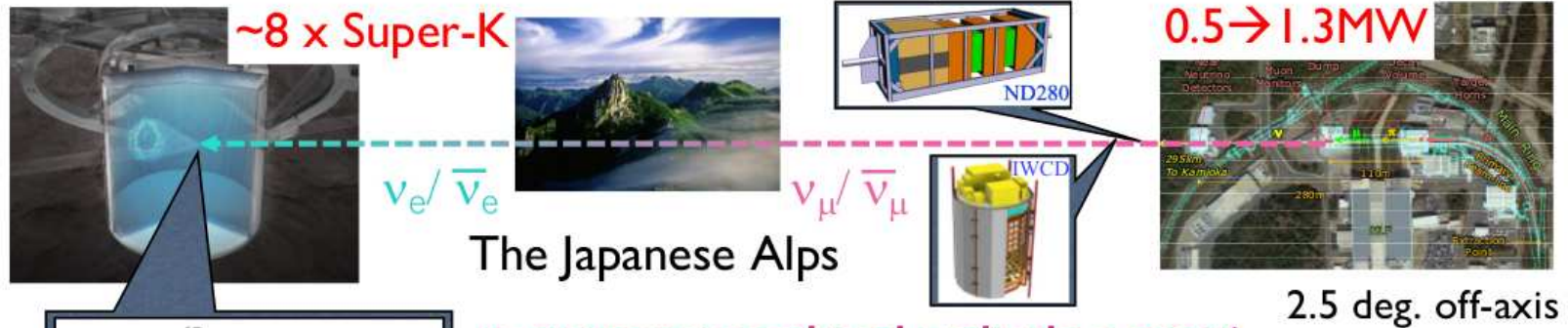
# Hyper-Kamiokande and T2HK

**Hyper-Kamiokande: water-Cherenkov,  $\sim 0.25$  Mton, fiducial  $\sim 0.2$  Mton; 2028; T2HK.**

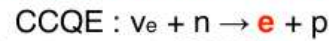


The next slides are from the talk by S. Muriyama at Neutrino 2024.

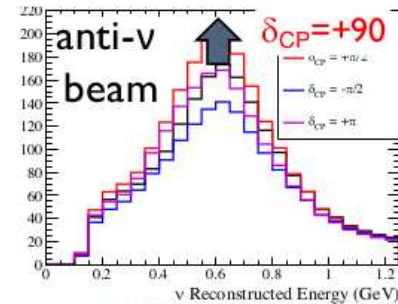
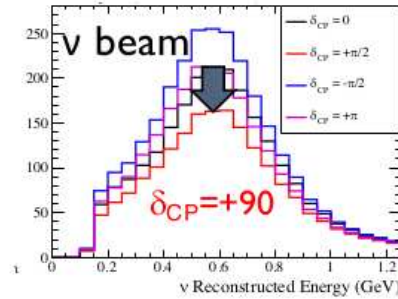
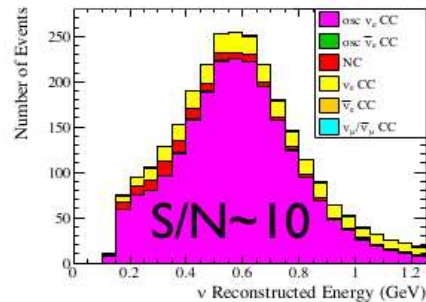
## J-PARC off-axis $\nu_\mu$ & $\bar{\nu}_\mu$ beam ( $\sim 0.6$ GeV, $\sim 295$ km)



$\nu_e$  appearance signal = single e event



(dominant process at J-PARC beam energy)



Relatively  
Small matter  
Effect &  
Large CPV  
Effect

HK 10 yr,  $2.7 \times 10^{22}$  POT 1:3  $\nu : \bar{\nu}$ , 1-ring e-like + 0 decay e, > 1000 events each



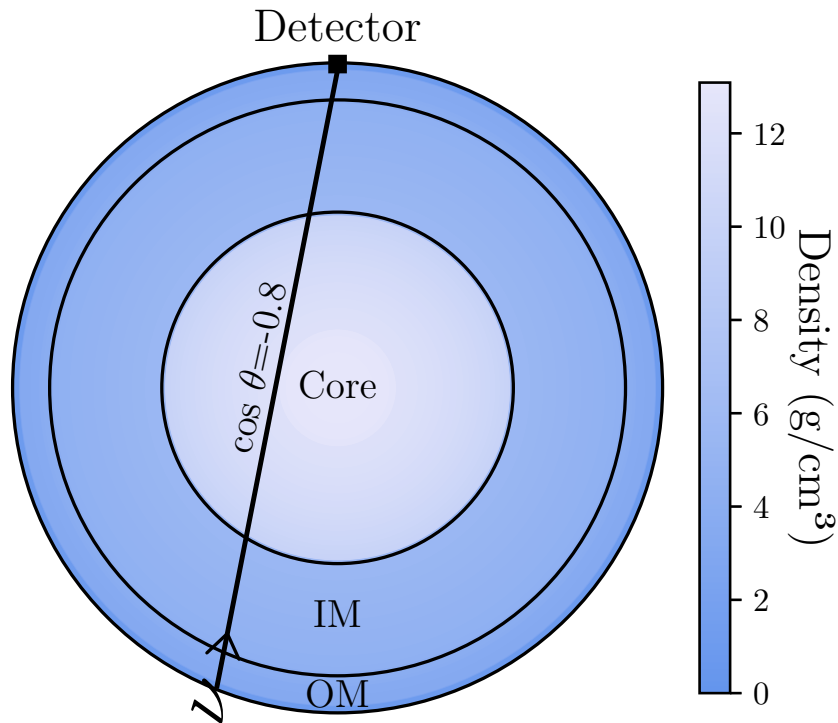
# Summary

- Hyper-K will play a central role in exploring the future of particle physics and contribute to the future of astronomy. Expectations in 10 yrs HK:
  - Mass ordering:  $3.8-6.2\sigma$  depending on  $\sin^2\theta_{23}$
  - CP violation:  $5\sigma$  discovery,  $> 60\%$
  - Proton decay:  $p \rightarrow e^+\pi^0$ :  $\sim 6 \times 10^{34}$  yrs etc.
  - $> 3\sigma$  sensitivity for the solar  $\nu$  spectrum up-turn
  - $\sim 70k$  events @10 kpc supernova
  - $\sim 4$  events/yr diffuse supernova neutrino background
- The highlight of the civil construction, the dome excavation, was completed. Detailed design of tank lining and photosensor support structure completed.
- 50 cm PMT delivery is ongoing and on schedule.
- Beam intensity increase/IWCD construction is on the way.
- Data-taking is expected to start in 2027!

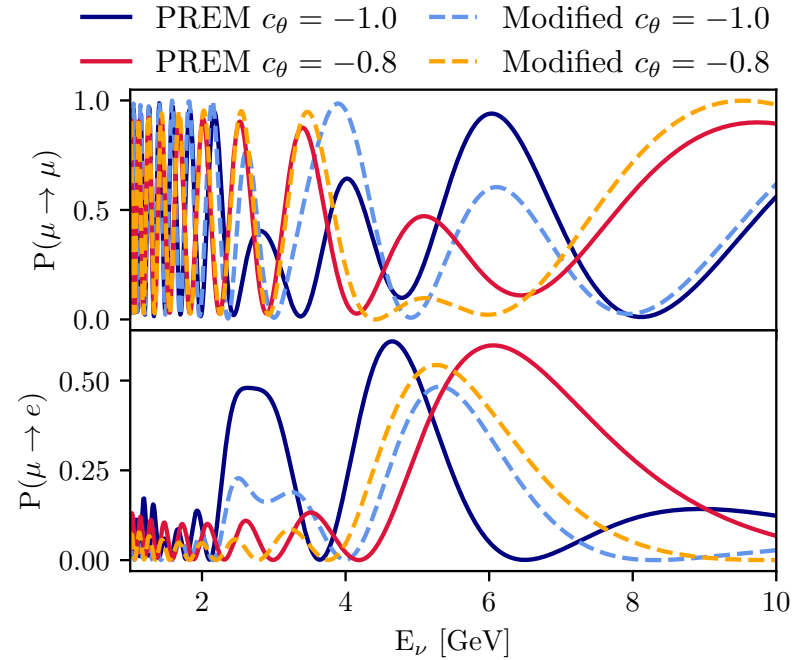
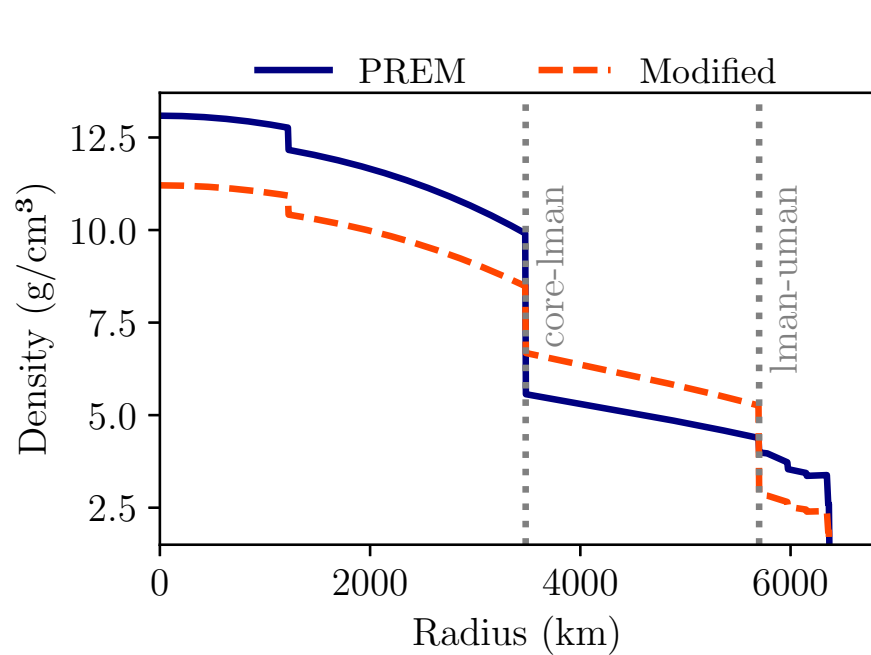
23

**Scheduled to star data-taking on April 1, 2028.**

# Aspects of the Analysis



A diagram of the Earth interior under study. The angle  $\cos \theta = -1$  corresponds to an up-going neutrino crossing the Earth along the diameter before being detected.



Left panel: Earth density according to PREM and an example solution for a modified Earth with fixed  $\kappa_{lman} = 0.2$ .

Right panel:  $\nu_\nu$  disappearance and  $\nu_e$  appearance probabilities for two values of the azimuth angle and the Earth models shown in the left panel.

## Analysis Methodology

This study uses the public release (Zenodo, Oct. 4, 2023. doi: 10.5281/zenodo.8401262) simulated atmospheric neutrino event rate predictions generated by the Super-Kamiokande (SK) collaboration in its latest atmospheric neutrino oscillation analysis (Phys. Rev. D 109 (2024) 072014 [arXiv:2311.05105]). It consists of the expected event rates, and one-dimensional true energy and angle event distributions for a list of 931 angle and energy bins divided in 29 samples, corresponding to 29 different sets of event selection conditions. The distributions are released as 1D true neutrino energy and true azimuth angle quantiles at 2.3%, 15.9%, 50%, 84.1% and 97.7% of the distribution. The predictions are divided in three major blocks, consisting of the unoscillated, and oscillated predictions assuming either the normal or the inverted mass ordering. For each, the predictions are divided in six components:  $\nu_e$ ,  $\nu_\mu$ ,  $\bar{\nu}_e$ ,  $\bar{\nu}_\mu$ ,  $\nu_\tau + \bar{\nu}_\tau$  and neutral current (NC). Additionally, the measured data counts in every bin are provided.

The 29 selections samples can be sub-divided in 19 samples without and 10 with neutron tagging, often indicated with additional labels 0 n, 1 n, etc. This large number of samples is the result, in part, to splitting some samples in two phases of the Super-Kamiokande experiment, i.e. data from SK runs 1 to 3 and from runs 4 to 5, further details on the specifics of this data periods are available in Phys. Rev. D 109 (2024) 072014 [arXiv:2311.05105].

Broadly speaking there are 4 different categories of samples: Sub-GeV

samples, Multi- GeV samples, NC-samples, and non-fully-contained (non-FC) samples. Oscillations of neutrinos with energy below 1 GeV change very rapidly with energy and azimuth angle, see previous Fig. 2, such that tomography-sensitive variations get largely averaged out. Therefore we do not consider Sub-GeV samples. Similarly, as our interest regards effects in the neutrino flux flavor composition, we do not include NC-samples, insensitive to flavor transitions. Lastly, we only consider those samples that have a significant fraction of events with energies of interest. Accordingly, we ignore the Up- $\mu$  showering and Up- $\mu$  stopping samples, which largely consist of events with energies above several tens of GeV.

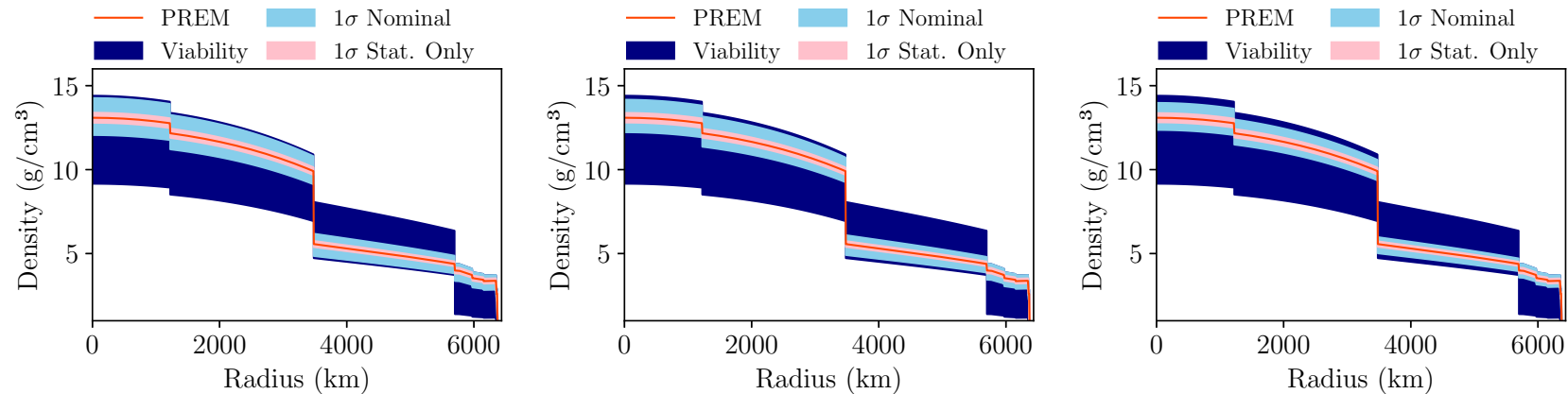
Therefore, in this analysis we utilize a total of 12 selection samples, consisting of Multi-GeV events with a single lepton ring ( $\nu_\mu, \bar{\nu}_\mu, \nu_e, \bar{\nu}_e$  0 n,  $\bar{\nu}_e$  1 n) and Multi-GeV events with multiple rings ( $\nu_\mu, \nu_e, \bar{\nu}_e$  and other), and non-FC events (partially contained stopping, partially contained through-going and Up- $\mu$  stopping).

Our analysis includes realistic flux (M. Honda et al., Phys. Rev. D83 (2011) 123001 [arXiv:1102.2688]), neutrino interaction modeling using NEUT (Y. Hayato, L. Pickering, EPJ ST 230 (2021) 4469), detector effects and analysis sample selection criteria. Based on those simulations, we extrapolate the Earth tomography sensitivity to Hyper-Kamiokande (HK), a detector eight times larger than SK, but based on the same detection concept and with small instrumentation differences. Additionally, we modify the nominal distributions to assess the potential impact of enhanced energy and/or angular resolutions in HK.

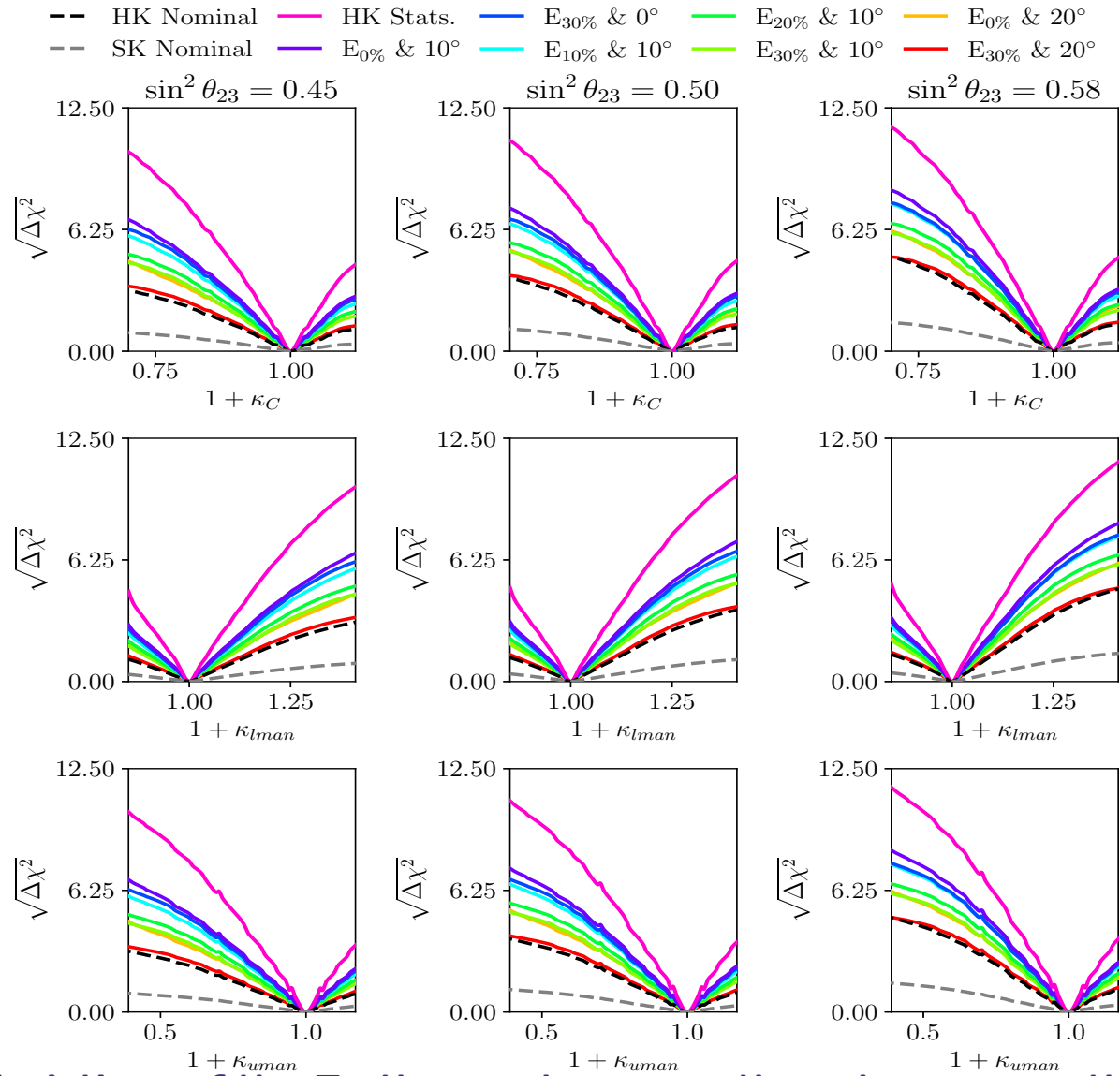
## Oscillation probability evaluation

The 3-flavour oscillation probability is evaluated using the `Prob3++` framework (for details see <https://github.com/rogerwendell/Prob3plusplus>), developed by Super-Kamiokande collaborators. The framework calculates the oscillation probability including matter effects for any neutrino flavor transition as a function of the input PMNS parameters, the values of the neutrino mass squared differences values, and the Earth model configuration, which is input as a collection of density values along the Earth radius. `Prob3++` takes as input the Earth density profile given by a collection of points. We evaluate the Earth density at 82 points along the Earth radius. A subset of 61 points are distributed from 0 to 5600 km every 100 km, with few additional points near the shell transitions. The remaining points describe the 5600 km to 6371 km region, sampled more frequently at irregular intervals to reflect the finer structure of the Earth crust.

# Results



Confidence intervals of HK sensitivity to deviations of the core, lower mantle and upper mantle average densities from their respective PREM values. The dark blue bands correspond to varying  $\kappa_C$  in the interval  $-0.30 < \kappa_C < 0.10$ , allowed by the Earth total mass, moment of inertia and hydrostatic equilibrium constraints. The light blue and red bands represent the  $1\sigma$  *Nominal* ( $E_{30\%}$  &  $20^\circ$ ) and *Stats.Only* ( $E_0$  &  $0^\circ$ ) confidence level intervals. The left, center and right panels correspond respectively to  $\sin^2 \theta_{23} = 0.45, 0.50, 0.58$ .



**Sensitivity to deviations of the Earth core, lower mantle and upper mantle densities from their respective PREM values, parametrised as  $\rho_i(1 + \kappa_i)$ ,  $i = c, lman, uman$ ,  $\rho_i$  being the PREM densities, for different HK detector configurations. The left, center and right columns correspond to:  $\sin^2 \theta_{23} = 0.45, 0.50$  and  $0.58$ .**

We find, in particular, that for  $\sin^2 \theta_{23} = 0.5$  and the “nominal” energy and zenith angle resolutions of  $E_{30\%}$  &  $20^\circ$  in all samples, after 6500 days of operation the HK experiment can determine the Earth core average density at  $2\sigma$  C.L. with a relative uncertainty

$$\Delta \bar{\rho}_C / \bar{\rho}_C = 100\% \kappa_C \text{ of } (-14.5\%) / +39.5 \text{ } (-0.145 \leq \kappa_c \leq 0.395).$$

For  $\sin^2 \theta_{23} = 0.58$  the uncertainty is noticeably smaller:  $(-9.3\%) / +31.7\%$  ( $-0.093 \leq \kappa_c \leq 0.317$ ).

The sensitivity of the HK experiment will be much higher in the case of energy and angular resolutions of  $E_{20\%}$  &  $10^\circ$ . It increases also significantly with  $\sin^2 \theta_{23}$ . Indeed, in this case at  $2\sigma$  C.L. we have **for  $\sin^2 \theta_{23} = 0.45, 0.50$  and  $0.58$ , respectively:  $(-9.2\%) / +11.3\%$  ( $-0.092 \leq \kappa_c \leq 0.113$ ),  $(-8.3\%) / +9.8\%$  ( $-0.083 \leq \kappa_c \leq 0.098$ ) and  $(-6.7\%) / +8.5\%$  ( $-0.067 \leq \kappa_c \leq 0.085$ )** .

Thus, if, e.g.,  $\sin^2 \theta_{23} = 0.50$ , the HK experiment would be able to establish that **the average core density at  $2\sigma$  C.L. lies in the rather narrow interval:  $10.08 \text{ g/cm}^3 \leq \bar{\rho}_C \leq 12.06 \text{ g/cm}^3$ , with the PREM value of  $\bar{\rho}_C = 10.99 \text{ g/cm}^3$ .**

Similarly, it will follow from the HK data that **at  $2\sigma$  C.L. the average lower and upper mantle densities, have values in the intervals:  $4.49 \text{ g/cm}^3 \leq \bar{\rho}_{lman} \leq 5.38 \text{ g/cm}^3$ ,  $3.00 \text{ g/cm}^3 \leq \bar{\rho}_{uman} \leq 4.25 \text{ g/cm}^3$  . We recall that the PREM values of  $\bar{\rho}_{lman}$  and  $\bar{\rho}_{uman}$  are  $4.90 \text{ g/cm}^3$  and  $3.60 \text{ g/cm}^3$ , respectively.**

**Given the PREM values of  $\bar{\rho}_{man} = 4.66 \text{ g/cm}^3$  and  $\bar{\rho}_{IC} = 12.89 \text{ g/cm}^3$ , the HK result on  $\bar{\rho}_C$  would be an independent confirmation of the existence of at least three major density layers in the interior of the Earth.**

## Conclusion

**Our results show that the Hyper-Kamiokande experiment, after collecting a sufficiently large data sample, can make a major contribution to the tomography studies of the Earth interior with neutrinos.**